

Structural and functional profile of phytases across the domains of life

Benjamin M. Scott^{a,*}, Kevin Koh^a, Gregory D. Rix^b

^a Global Institute for Food Security, University of Saskatchewan, 421 Downey Road, S7N 4L8, Saskatoon, Saskatchewan, Canada

^b Inspiralis Ltd., Innovation Centre, Norwich Research Park, Colney Lane, NR4 7UH, Norwich, UK

ARTICLE INFO

Handling Editor: Prof G Oliva

ABSTRACT

Phytase enzymes are a crucial component of the natural phosphorus cycle, as they help make phosphate bioavailable by releasing it from phytate, the primary reservoir of organic phosphorus in grain and soil. Phytases also comprise a significant segment of the agricultural enzyme market, used primarily as an animal feed additive. At least four structurally and mechanistically distinct classes of phytases have evolved in bacteria and eukaryotes, and the natural diversity of each class is explored here using advances in protein structure prediction and functional annotation. This graphical review aims to provide a succinct description of the major classes of phytase enzymes across phyla, including their structures, conserved motifs, and mechanisms of action.

1. Introduction

Phytases catalyse the stepwise release of phosphate from phytic acid (myo-inositol hexakisphosphate; InsP₆) and from its anionic salt phytate. Comprised of an inositol carbon ring and six phosphate groups, phytic acid is primarily in the phytate form at physiological pH, which readily forms stable complexes with metal cations (i.e. calcium, iron, magnesium, zinc). Phytate is the primary molecule that plants use to store phosphorus, comprising >90% of phosphorus in seeds and between 20% and 80% of organic phosphorus in soil and manure (Liu et al., 2022). Despite its relative abundance in nature, plants and animals cannot directly absorb phytate to harness the associated phosphorus, which may be due to its stable negatively charged structure. The action of phytases expressed by microbes in the soil and guts of ruminants, in addition to organic acids secreted by plant roots, are therefore crucial to making this abundant source of phosphorus bioavailable.

Monogastric animals including humans, poultry, swine, and fish, do not contain phytase-expressing microbes in their guts, resulting in poor phosphorus uptake from their grain-based diets (Greiner and Konietzny, 2006). This causes significant phytate accumulation in animal manure (39–80% P_o, 16–17% P_f), which leads to water eutrophication when it runs off fields (Liu et al., 2022). The chelating effect of phytate also binds dietary minerals, reducing their absorption in the gut, and phytate has consequently been deemed an anti-nutritive (Greiner and Konietzny, 2006). To address these issues, phytases have been used for over 30 years to treat plant-based animal feeds, particularly for swine and poultry (Herrmann et al., 2019; Selle et al., 2009). In addition to the

release of more bioavailable phosphorus from seed grains, phytases increase the bioavailability of minerals, and improve protein and starch digestion (Greiner and Konietzny, 2006; Selle et al., 2009, 2023). Many commercial phytases are available representing a >\$350 M global market, which are bacterial or fungal in origin and typically expressed recombinantly using a fungal host, (Herrmann et al., 2019). Phytases have also been proposed as human food additives for similar reasons, and also to enhance fertilizer efficiency by increasing the bioavailability of phosphorus in soil (Herrmann et al., 2019; Liu et al., 2022).

Many different phytase enzymes have evolved and are primarily expressed by bacteria, fungi, and plants. Animal phytases are also important for the regulation of myo-inositol and its various derivatives, which are important cell signaling molecules (Su et al., 2023). Phytases can be broadly categorised into four structurally distinct classes: Histidine Acid Phytases (HAPhys), β-Propeller Phytases (BPPhys/alkaline phytases), Protein Tyrosine Phosphatase-like phytases (PTPhys/cysteine phytases), and Purple Acid Phytases (PAPhys). Each class has a unique catalytic mechanism and different trends in stability, and optimal pH/temperature. Building on recent advances in protein structure prediction and functional annotation, we present a structure-function based overview of phytases from across phyla.

2. Histidine acid phytases

Histidine acid phytases (HAPhys) are part of clade 2 of the histidine acid phosphatase superfamily (HP2) and are the largest and most widely studied class of phytases. HAPhys are primarily bacterial and fungal in

* Corresponding author.

E-mail address: ben.scott@gifs.ca (B.M. Scott).

<https://doi.org/10.1016/j.crstbi.2024.100139>

Received 15 December 2023; Received in revised form 3 March 2024; Accepted 19 March 2024

Available online 20 March 2024

2665-928X/© 2024 The Authors. Published by Elsevier B.V. This is an open access article under the CC BY-NC-ND license (<http://creativecommons.org/licenses/by-nc-nd/4.0/>).

origin (Fig. 1A) and can be sorted into two clades: histidine acid phosphatases with phytase activity (HP2Ps), and the subclade multiple inositol polyphosphate phosphatases (MINPPs) (Acquistapace et al., 2020). HAPhys can hydrolyse a total of five phosphate groups from InsP₆, eventually yielding myo-inositol 2-monophosphate, although they have reduced affinity for lower InsP species (Herrmann et al., 2019; Wyss et al., 1999). The conserved active site motif RHGxRxP is found in all HAPhys, while HP2Ps contain the catalytic motif HD and MINPPs contain HAE, where the acidic residue in both cases acts as a proton donor that breaks the phosphomonoester bond, releasing a phosphate group from phytate (Acquistapace et al., 2020). As the name suggests, MINPPs have a wide range of substrates with activity towards many other phosphate containing molecules, and with less stereospecificity for the initial phosphate hydrolysis from InsP₆ versus HP2Ps (Acquistapace et al., 2020; Stentz et al., 2014).

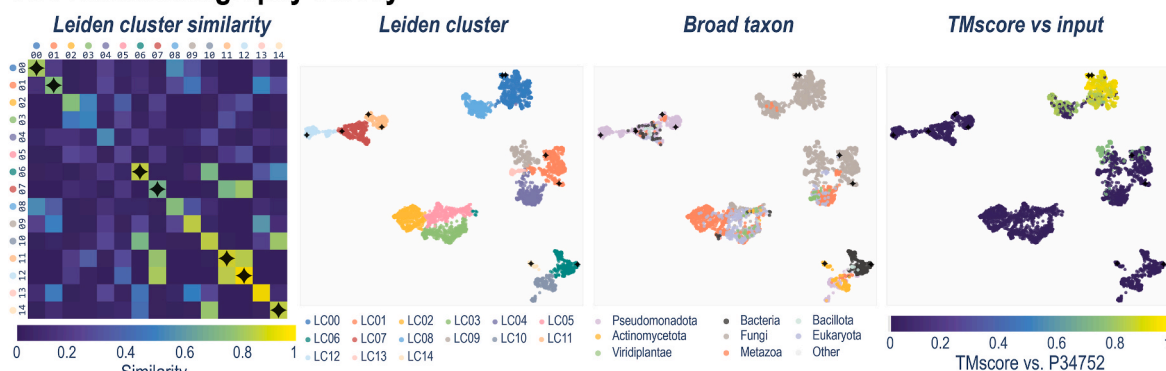
HAPhys contain two general structural domains, α/β and α (Fig. 1B), with a positively charged substrate binding pocket located between them optimised for binding negatively charged phytate. Metal cations therefore disrupt HAPhys activity, by chelating phytate which reduces electrostatic interactions with the substrate binding pocket (Wyss et al., 1999). HAPhys also contain a variable N-terminal region, larger amongst fungal HAPhys, which can include a short signal peptide or motifs involved in multimer formation (Chen et al., 2015). The α/β -domain is structurally conserved across HP2 proteins, consisting of a

5- to 6-stranded β -sheet sandwiched between two sets of α -helices. The α -domain is more variable, with fungal HAPhys generally containing a smaller, more structured, and therefore less flexible α -domain compared to other eukaryotic HP2s and bacterial HAPhys (Fig. S1). This structural plasticity of the α -domain contributes to sequence-specific differences in substrate specificity, evidenced by recent mutagenesis and directed evolution studies (Acquistapace et al., 2020, 2022; Herrmann et al., 2022; Rix et al., 2022). In particular, some bacterial MINPPs contain a large α -domain insertion named the U-loop, which forms a lid that undergoes significant movement during substrate binding (Acquistapace et al., 2020). Deeper analysis of our ProteinCartography survey, which grouped phytases based on structural similarities, revealed that HAPhys were clustered primarily based on these differences between the structures of the α -domain (Fig. S1). U-loop insertions in the α -domain were observed in at least 148 sequences clustered in LC10 and LC14, from various *Bifidobacterium*, *Burkholderia*, and *Acinetobacter* species among others (manually annotated in Table S1).

HAPhys have the highest specific activity across the four classes of phytases, ranging from 50 to >3000 U/mg under optimal conditions (Greiner and Konietzny, 2006), with bacterial HAPhys displaying greater specific activity versus fungal HAPhys that may be due to their more flexible substrate binding site (Shivange and Schwaneberg, 2017). HAPhys are thus of significant commercial interest as animal feed additives due to high catalytic activity, in addition to typically having a

Histidine Acid Phytases (HAPhys)

A. ProteinCartography survey



B. Representative example

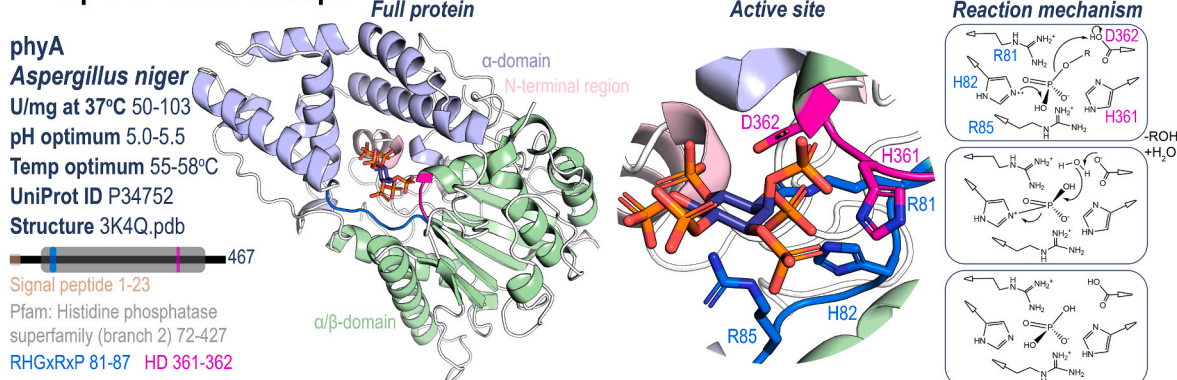


Fig. 1. Histidine Acid Phytases (HAPhys) A. HAPhys from fungi (P34752, O00092, P34755, A2TB4) and bacteria (B7GTV0, Q89Y18, Q84CN9, P07102, H9TUK5, H9TUK6) were used as input for the ProteinCartography tool, indicated by \blacklozenge . Based on structural similarities, known and putative phytases/phosphatases grouped into 14 Leiden clusters, which approximately correspond to fungal HP2P (LC00, LC01), bacterial HP2P (LC07, LC11, LC12), bacterial MINPP clade 1 (LC06), and bacterial MINPP clade 2 (LC10, LC14) (Acquistapace et al., 2020). B. Positively charged residues in the substrate binding pocket of HAPhys, including the highly conserved RHGxRxP motif, form favourable electrostatic interactions with the negatively charged phosphate groups of phytate. The catalytic H82 residue acts as a nucleophile, which attacks a phosphate group on phytate. D362 acts as a proton donor, breaking the phosphomonoester bond and replacing the lost phosphate with an alcohol group on the inositol ring. Now negatively charged, the D362 residue attacks a water molecule, which then attacks and releases the phosphohistidine intermediate. The enzyme active site is thus regenerated and inorganic phosphate is released. Mechanism from (Kostrewa et al., 1997), activity and temperature/pH optimums from (Greiner and Konietzny, 2006).

high temperature optima (50–60 °C) and a pH optima usually in the acidic range which enables optimal function in the gut and during animal feed processing (Greiner and Konietzny, 2006; Herrmann et al., 2019). A variety of protein engineering efforts have sought to increase HAPhy stability, increase activity towards lower species of InsP, or shift the optimal pH range (Herrmann et al., 2019, 2022).

3. β -propeller phytases

β -propeller phytases (BPPHys), also referred to as alkaline phytases due to their more basic optimal pH range versus HAPHys, contain the prototypical β -propeller fold comprised of a ring of six β -sheets (Fig. 2B). Counterintuitively, BPPHys contain an acidic active site, with highly conserved DAADDPAIW and NNVD motifs that function to bind calcium cations. It is the interaction of the positively charged calcium with negatively charged phytate, in concert with a proton donated by a water molecule or basic amino acid, that hydrolyses phosphate. BPPHy activity is therefore calcium dependent, and the binding of calcium also imbues this class of phytase with high thermostability via stabilizing interactions with the aforementioned motifs (Shin et al., 2001).

BPPHys can only release every other phosphate from InsP₆, eventually forming Ins(2,4,6)P₃, due to staggered phosphate-binding and phosphate-hydrolysing pockets (Oh et al., 2006; Shin et al., 2001). This unique structure and reaction mechanism makes BPPHys highly specific to phytate and typically have greater activity towards calcium-phytate versus HAPHys (Herrmann et al., 2019; Shin et al., 2001). These properties are relevant to agricultural applications of BPPHys as

calcium-phytate is readily found in alkaline soil, and calcium-phytate is not readily hydrolysed by phytases currently used as feed additives (Liu et al., 2022; Selle et al., 2009). However, BPPHys have not yet been commercialised.

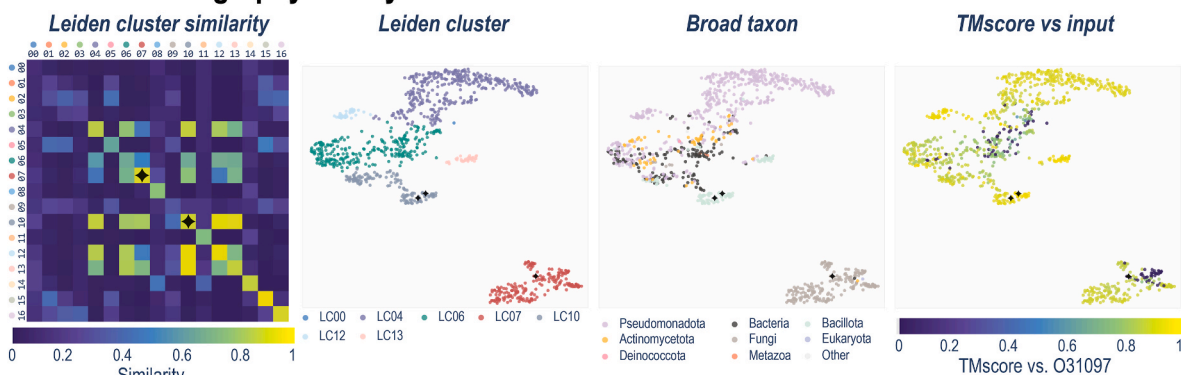
BPPHys have primarily been identified in bacteria, with BPPHys from *Bacillus* species the most well characterized (Fig. 2A). A fungal BPPHy was recently identified which contains a tandem repeat structure (β -propeller-linker- β -propeller) and ~5-fold greater phytase activity versus bacterial BPPHys (Hou et al., 2020). Over 200 structurally similar fungal proteins were identified using ProteinCartography (Fig. 2A), suggesting there are many other fungal BPPHys yet to be characterized. Interestingly, the tandem repeat structure among BPPHys appeared well conserved across phyla, particularly in LC04, LC07, and LC12 (Fig. S2; manually annotated in Table S1). In these tandem repeat BPPHys, the C-terminal β -propeller contained the phytase active site with high sequence conservation, while the N-terminal β -propeller sequence was poorly conserved with no consistent Pfam, indicative of functional divergence.

4. Protein tyrosine phosphatase-like phytases

The complex gut microbiome of ruminants is capable of degrading dietary phytate, enabling them to access the associated phosphate content for nutrition (Yanke et al., 1998). Among the enzymes responsible are protein tyrosine phosphatase-like phytases (PTPHys), also known as cysteine phytases due to the identity of the catalytic residue, which were first identified in the anaerobic ruminant bacterial species

β -Propeller Phytases (BPPHys)

A. ProteinCartography survey



B. Representative example

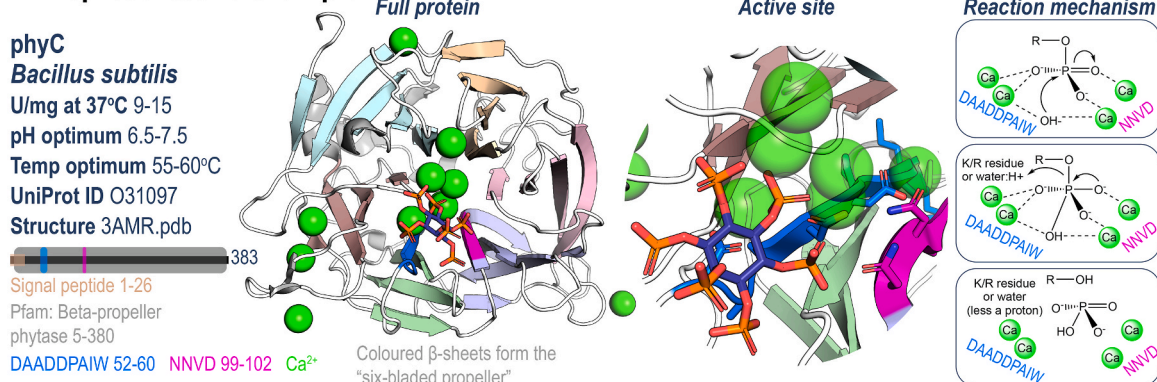


Fig. 2. β -Propeller Phytases (BPPHys) A. BPPHys from bacteria (O66037, O31097) and fungi (G1XN29) were used as input for the ProteinCartography tool, indicated by \blacklozenge . Based on structural similarities, known and putative phytases/phosphatases grouped into 16 Leiden clusters. 7 Leiden clusters are highlighted, as the remaining 9 clusters contain unrelated proteins with a β -propeller fold. B. Calcium cations coordinated by the conserved DAADDPAIW and NNVD motifs form bridging interactions with an activated water group, which attacks a bound phosphate. The phosphate group is then released through the action of a basic amino acid residue or water molecule, which functions as a general acid. Mechanism from (Shin et al., 2001), activity and temperature/pH optimums from (Greiner and Konietzny, 2006).

S. ruminantium. PTPHys have only been identified in bacteria and from environmental samples that are likely of bacterial origin (Castillo Villamizar et al., 2019b), but share structural homology with the Paladin protein tyrosine phosphatases found in plants and animals (Fig. 3A; Fig. S3) (Alonso and Pulido, 2016).

PTPHys are generally comprised of a partial β -barrel domain, and a larger protein tyrosine phosphatase (PTP) core domain formed by a parallel β -sheet and multiple α -helices (Fig. 3B). PTPHys contain the characteristic PTP sequence motif CxxxxR within the P-loop of the active site, where the catalytic cysteine functions as a nucleophile, and the aspartate of the nearby WPD-loop (also called the general acid (GA) loop) acts as the proton donor which completes the release of phosphate from phytate (Puhl et al., 2007). PTPHys are generally most active at pH 4–5.5, and show a range of substrate specificity, with phytase activity ranging from 4 U/mg to >600 U/mg (Castillo Villamizar et al., 2019c; Puhl et al., 2007). Similar to HAPHys, the substrate binding pocket of PTPHys is enriched in positively charged residues, but the size of this pocket ranges among PTPHys (Grüniger et al., 2014). For example, PTPHy from *B. bacteriovorus* contains a small and deep substrate binding pocket specific to phytate, versus other PTPHys and related protein tyrosine phosphatases that are more promiscuous (Grüniger et al., 2014).

Interestingly, the tandemly repeated PTPHy from *M. multacida* contains two active sites with varying substrate specificities, with one active site skewed towards hydrolysis of lower InsP species (Grüniger et al.,

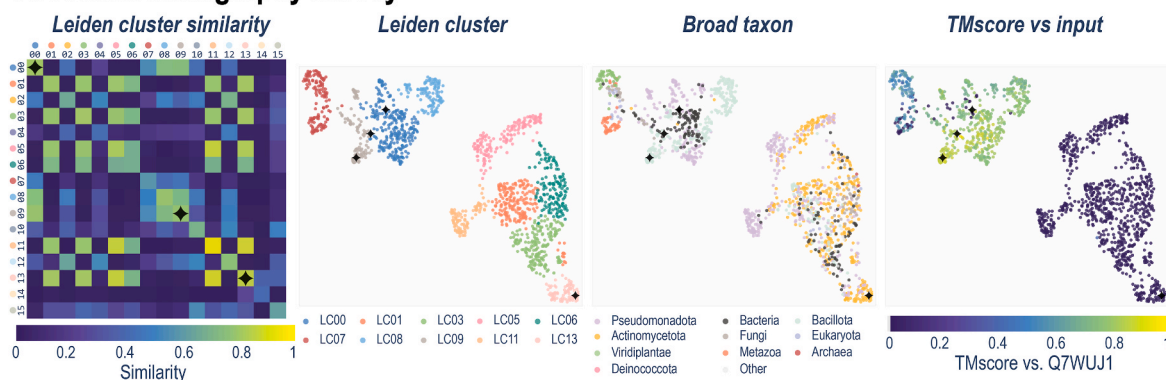
2009). Unlike BPPHys, this tandem repeat structure appeared to be rare amongst PTPHys, found in only three other sequences which includes one from another *M. multacida* strain (manually annotated in Table S1). The PTPHys substrate binding site conformation is rigid during product formation, but there are several long loops within the core PTP domain that affect substrate specificity (Bruder et al., 2017). Although these loops do not appear to directly interact with phytate, short loops within the PTP domain result in a more open binding pocket, resulting in many different InsP₄ species being generated from InsP₅ hydrolysis. Conversely, extensions of these loops “occlude” the active site, sterically hindering the formation of certain InsP₄ products depending on which loop extension is present. Despite favourable catalytic activity, and this apparent ability to tune substrate specificity, PTPHys have not been developed into a commercial product, which may be because like other PTP proteins PTPHys can be irreversibly inactivated through the oxidation of the catalytic cysteine residue (Grüniger et al., 2008).

5. Purple acid phytase

Purple acid phytases (PAPHys) belong to the metallophosphoesterase (MPE) superfamily and earned their colourful name due to their appearance when their iron core is oxidised (Schenk et al., 2013). Plant PAPHys have been the most widely characterized but PAPHys have also been identified in fungi and bacteria (Fig. 4A) (Castillo Villamizar et al., 2019b; Dionisio et al., 2011; Ullah and Cummins, 1988). PAPHys from

Protein Tyrosine Phosphatase-like Phytases (PTPHys)

A. ProteinCartography survey



B. Representative example

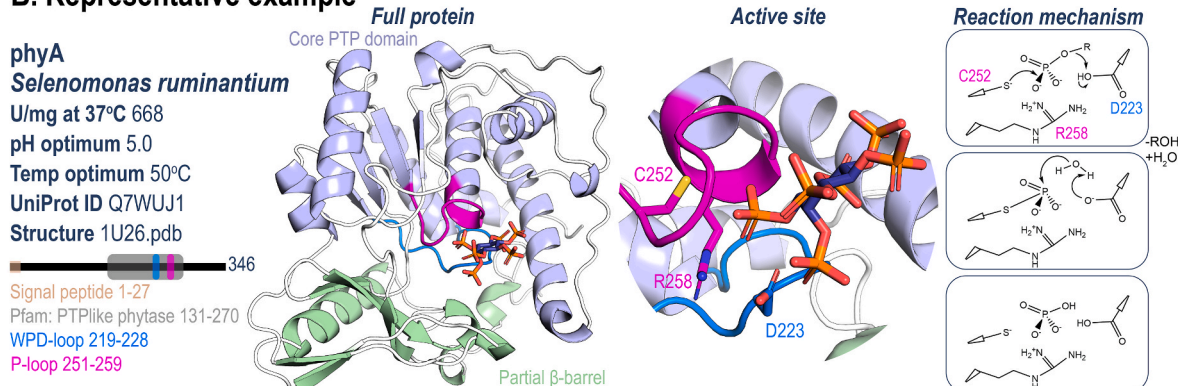
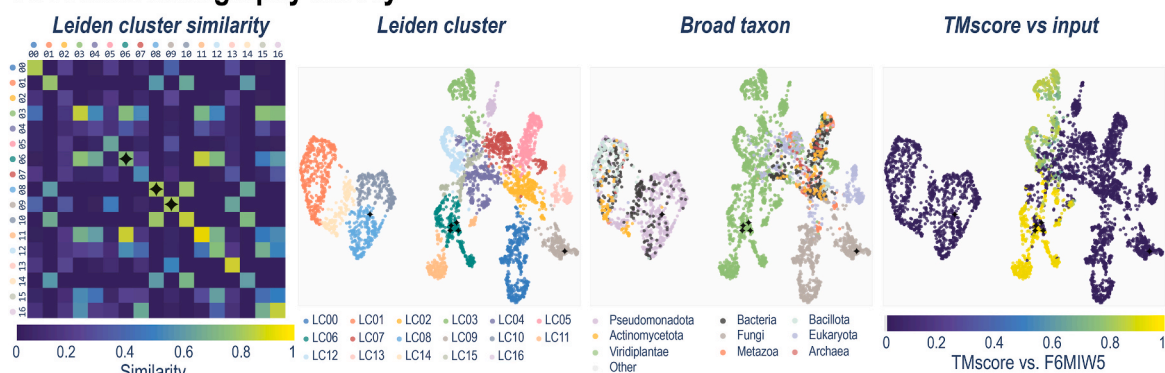


Fig. 3. Protein Tyrosine Phosphatase-like Phytases (PTPHys) A. PTPHys from bacteria (A3QMF6, Q7WUJ1, Q6MNP0) and an environmental sample likely of bacterial origin (A0A3G1QTG4) were used as input for the ProteinCartography tool, indicated by \star . Based on structural similarities, known and putative phytases/phosphatases grouped into 15 Leiden clusters. 10 Leiden clusters are highlighted, as the remaining 5 clusters contain unrelated protein tyrosine phosphatases. A0A3G1QTG4 (LC13) is predicted to contain a larger β -barrel domain compared to the partial β -barrel found in the other three input proteins (LC00, LC09). B. PTPHys contain a positively charged active site, including R258, which binds negatively charged phytate. The thiolate anion of the catalytic cysteine residue then attacks a phosphate group, generating a phosphocysteine intermediate. An acidic residue on the WPD-loop (D223) acts as a general acid by donating a proton, breaking the phosphoester bond. D223 then takes a proton from a bound water molecule which in turn attacks the phosphocysteine intermediate, releasing the phosphate and resetting the catalytic system. Mechanism from (Chu et al., 2004), activity and temperature/pH optimums from (Puhl et al., 2007).

Purple Acid Phytases (PAPhys)

A. ProteinCartography survey



B. Representative example

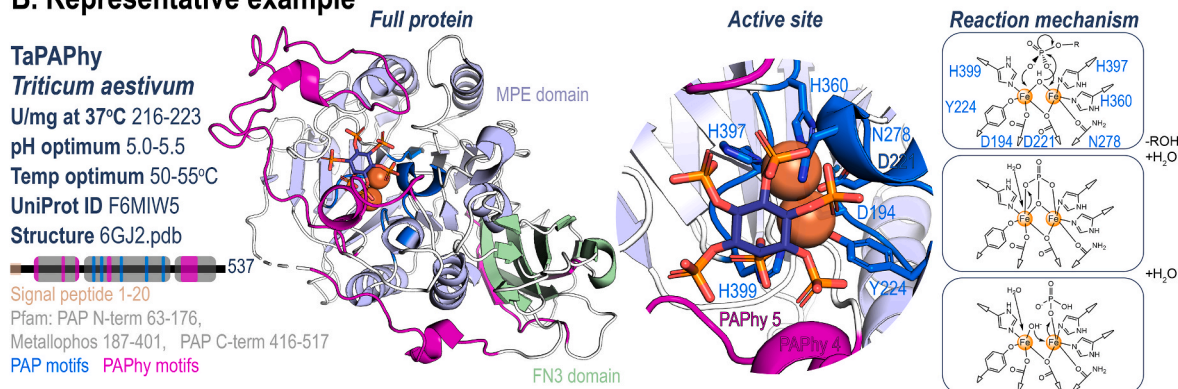


Fig. 4. Purple Acid Phytases (PAPhys) A. PAPhys from plants (F6MIW5, C4PKL2, C4PKL6, Q84JJ6), fungi (A2R1M4), and an environmental sample likely of bacterial origin (A0A3G1QTG2) were used as input for the ProteinCartography tool, indicated by \star . Based on structural similarities, known and putative phytases/phosphatases grouped into 16 Leiden clusters. The plant PAPhys cluster closely together indicating high structural similarity (LC06), while A2R1M4 contains the FN3 and MPE domains but lacks the PAPHy motifs (LC09). A0A3G1QTG2 does not contain the PAP N-term and C-term regions and instead clustered with smaller PAP2 proteins (LC08). B. A phosphate group on phytate binds to the iron ions, which is stabilized by the PAP motifs. A metal-bound hydroxide attacks the phosphate group, which breaks the phosphomonoester bond and forms a hydroxyl group on phytate, leaving behind phosphate. The bound phosphate is then released through the action of two water molecules, which regenerates the catalytic mechanism. A more detailed multi-step reaction mechanism is described by (Schenk et al., 2013), activity and temperature/pH optimums from (Dionisio et al., 2011). (For interpretation of the references to colour in this figure legend, the reader is referred to the Web version of this article.)

plants and fungi contain a fibronectin-like FN3 domain and MPE domain and are most active at pH 5.0–6.0 (Fig. 4B) (Dionisio et al., 2011; Faba-Rodriguez et al., 2022). The bacterial PAPhy was isolated from an environmental sample, and is more closely related to type-2 phosphatidic acid phosphatases (PAP2), and lacks the FN3 domain entirely (Castillo Villamizar et al., 2019b).

In our analysis of the ProteinCartography results, PAPhys did not appear as a structurally distinct clade unto themselves, meaning they were intermixed with and difficult to distinguish from structurally similar phosphatases that have different substrate preferences. The FN3 domain, a small β sandwich, was less conserved across proteins captured by the ProteinCartography survey (Fig. S4), suggesting it is not crucial for phosphatase activity. This is not surprising, given that the active site is in the MPE domain, which contains two metal cations coordinated by highly conserved PAP motifs (Schenk et al., 2013). These PAP motifs (GDxxY, GNHE, GHxH, GDxG, V/AxxH) contain several polar residues essential for coordinating the metal ions and are therefore crucial for the function of PAPhys (Fig. 4B). The MPE domain overall folds in a α/β sandwich structure, with the PAP motifs located at the C-terminal ends of the β -sheet.

Plant PAPhys additionally contain up to five conserved PAPHy motifs which form an “electropositive horseshoe-shaped collar” around the otherwise negatively charged active site (Faba-Rodriguez et al., 2022). Similar to HAPHys and PTPHys, this positively charged region forms

favourable electrostatic interactions with the phosphate groups on phytate. In particular, a histidine residue in PAPHy motif 4 is linked to phytase activity (Faba-Rodriguez et al., 2022), and was observed only in proteins in LC04, LC06, LC11, and LC15 which suggests these clusters may be enriched for phytases versus more generalist purple acid phosphatases (Fig. S4; manually annotated in Table S1).

6. Summary

Phytate’s significant negative charge and its propensity to chelate metal cations makes it a challenging enzyme substrate. That phytases utilise four unique catalytic mechanisms each with unrelated protein structures, underscores the innate power of enzyme evolution to overcome this challenge and the crucial role that phytases play in nature by releasing bioavailable phosphorus from an otherwise recalcitrant source. Known phytases across the four classes were input into the ProteinCartography tool (Avasthi et al., 2023), which performed a structure-based search to identify functionally similar proteins, providing a glimpse of the broad natural diversity of phytases and other phosphatases.

There are several important caveats to the ProteinCartography survey. The Leiden clusters reported here are inherently biased by the original input sequences and available structural/sequence information, and they do not necessarily represent phylogenetic or functional

relationships. Also, the distances between points on the 2D uniform manifold approximation projection (UMAP) plots are also not quantitative (Figs. 1-4A). Nevertheless, unique structural trends within Leiden clusters of the four classes of phytases could be observed, made more apparent by using the SSDraw tool (Chen and Porter, 2023). These structural trends appeared to correspond to some of the characterized functional subclades (i.e. HP2Ps and MINPPs), as well as previously unreported trends such as differences between plant PAPhys, and the identification of potential fungal BPPhys. Although only bacterial and eukaryotic phytases have been characterized so far, the recent report of metallo- β -lactamases with phytase activity may lead to the eventual discovery of archaeal phytases (Castillo Villamizar et al., 2019a).

It is our hope that this graphical review will be useful for scientists first learning about the various structures and functions of phytases, and also useful for experts wishing to mine this significant natural diversity for desired function. Given the potential economic and environmental potential of phytases, further study of natural sequences and their engineering for desired function is warranted.

CRediT authorship contribution statement

Benjamin M. Scott: Conceptualization, Data curation, Visualization, Writing – original draft. **Kevin Koh:** Software, Data curation, Visualization, Writing – review & editing. **Gregory D. Rix:** Resources, Writing – review & editing.

Declaration of competing interest

The authors declare that they have no known competing financial interests or personal relationships that could have appeared to influence the work reported in this paper.

Data availability

Data will be made available on request.

Acknowledgments

The ProteinCartography tool was created by Arcadia Science (Avasthi et al., 2023). 2D representations of secondary structures were generated using SSDraw (Chen and Porter 2023), using the indicated sequences and AlphaFold structures obtained from UniProt. Signal peptides and Pfam were annotated with HMMER and UniProt (Potter et al., 2018). Amino acid numbering maintains the presence of the signal peptide, although it is cleaved during subcellular localisation/secretion. An inflexible myo-inositol hexakisphosphate (phytate) molecule from 1DKQ.pdb was docked to phytase structures using AutoDock Vina 1.2.3 (Eberhardt et al., 2021) via the Webina webserver (Kochnev et al., 2020). Publication quality images were generated using PyMOL 2.5.5 and ChemDraw 22.2. This research did not receive any specific grant from funding agencies in the public, commercial, or not-for-profit sectors.

Appendix A. Supplementary data

Supplementary data to this article can be found online at <https://doi.org/10.1016/j.crstbi.2024.100139>.

References

Acquistapace, I.M., Thompson, E.J., Kühn, I., Bedford, M.R., Brearley, C.A., Hemmings, A.M., 2022. Insights to the structural basis for the stereospecificity of the *Escherichia coli* phytase, AppA. *Int. J. Mol. Sci.* 23 (11), 6346.
 Acquistapace, I.M., Ziętek, M.A., Li, A.W.H., Salmon, M., Kühn, I., et al., 2020. Snapshots during the catalytic cycle of a histidine acid phytase reveal an induced-fit structural mechanism. *J. Biol. Chem.* 295 (51), 17724–17737.

Alonso, A., Pulido, R., 2016. The extended human PTpome: a growing tyrosine phosphatase family. *FEBS J.* 283 (8), 1404–1429.
 Avasthi, P., Bigge, B.M., Celebi, F.M., Gehring, J., McGeev, E., et al., 2023. ProteinCartography: comparing proteins with structure-based maps for interactive exploration. *Arcadia Sci.*
 Bruder, L.M., Gruninger, R.J., Cleland, C.P., Mosimann, S.C., 2017. Bacterial PhyA protein-tyrosine phosphatase-like myo-inositol phosphatases in complex with the Ins(1,3,4,5)P₄ and Ins(1,4,5)P₃ second messengers. *J. Biol. Chem.* 292 (42), 17302–17311.
 Castillo Villamizar, G.A., Funkner, K., Nacke, H., Foerster, K., Daniel, R., 2019a. Functional metagenomics reveals a new catalytic domain, the metallo- β -lactamase superfamily domain, associated with phytase activity. *mSphere* 4 (3), e00167, 19.
 Castillo Villamizar, G.A., Nacke, H., Boehning, M., Herz, K., Daniel, R., 2019b. Functional metagenomics reveals an overlooked diversity and novel features of soil-derived bacterial phosphatases and phytases. *mBio* 10 (1). <https://doi.org/10.1128/mbio.01966-18>.
 Castillo Villamizar, G.A., Nacke, H., Griese, L., Taberner, L., Funkner, K., Daniel, R., 2019c. Characteristics of the first protein tyrosine phosphatase with phytase activity from a soil metagenome. *Genes* 10 (2), 101.
 Chen, C.-C., Cheng, K.-J., Ko, T.-P., Guo, R.-T., 2015. Current progresses in phytase research: three-dimensional structure and protein engineering. *ChemBioEng Rev.* 2 (2), 76–86.
 Chen, E.A., Porter, L.L., 2023. SSDraw: Software for generating comparative protein secondary structure diagrams. *Protein Sci.* 32 (12), e4836.
 Chu, H.-M., Guo, R.-T., Lin, T.-W., Chou, C.-C., Shr, H.-L., et al., 2004. Structures of selenomonas ruminantium phytase in complex with persulfated phytate. *Structure* 12 (11), 2015–2024.
 Dionisio, G., Madsen, C.K., Holm, P.B., Welinder, K.G., Jørgensen, M., et al., 2011. Cloning and characterization of purple acid phosphatase phytases from wheat, barley, maize, and rice[W][OA]. *Plant Physiol.* 156 (3), 1087–1100.
 Eberhardt, J., Santos-Martins, D., Tillack, A.F., Forli, S., 2021. AutoDock Vina 1.2.0: new docking methods, expanded force field, and Python bindings. *J. Chem. Inf. Model.* 61 (8), 3891–3898.
 Faba-Rodríguez, R., Gu, Y., Salmon, M., Dionisio, G., Brinch-Pedersen, H., et al., 2022. Structure of a cereal purple acid phytase provides new insights to phytate degradation in plants. *Plant Commun* 3 (2), 100305.
 Greiner, R., Konietzny, U., 2006. Phytase for food application. *Food Technol. Biotechnol.* 44 (2), 125–140.
 Gruninger, R.J., Selinger, L.B., Mosimann, S.C., 2008. Effect of ionic strength and oxidation on the P-loop conformation of the protein tyrosine phosphatase-like phytase, PhyAsr. *FEBS J.* 275 (15), 3783–3792.
 Gruninger, R.J., Selinger, L.B., Mosimann, S.C., 2009. Structural analysis of a multifunctional, tandemly repeated inositol polyphosphatase. *J. Mol. Biol.* 392 (1), 75–86.
 Gruninger, R.J., Thibault, J., Capeness, M.J., Till, R., Mosimann, S.C., et al., 2014. Structural and biochemical analysis of a unique phosphatase from *Bdellovibrio bacteriovorus* reveals its structural and functional relationship with the protein tyrosine phosphatase class of phytase. *PLoS One* 9 (4), e94403.
 Herrmann, K.R., Brethauer, C., Siedhoff, N.E., Hofmann, I., Eyll, J., et al., 2022. Evolution of *E. coli* phytase toward improved hydrolysis of inositol tetraphosphate. *Front. Chem. Eng.* 4.
 Herrmann, K.R., Ruff, A.J., Infanzón, B., Schwaneberg, U., 2019. Engineered phytases for emerging biotechnological applications beyond animal feeding. *Appl. Microbiol. Biotechnol.* 103 (16), 6435–6448.
 Hou, X., Shen, Z., Li, N., Kong, X., Sheng, K., et al., 2020. A novel fungal beta-propeller phytase from nematophagous *Arthrobotrys oligospora*: characterization and potential application in phosphorus and mineral release for feed processing. *Microb. Cell Factories* 19 (1), 84.
 Kochnev, Y., Hellemann, E., Cassidy, K.C., Durrant, J.D., 2020. Webina: an open-source library and web app that runs AutoDock Vina entirely in the web browser. *Bioinformatics* 36 (16), 4513–4515.
 Kostrewa, D., Grüniger-Leitch, F., D'Arcy, A., Broger, C., Mitchell, D., van Loon, A.P., 1997. Crystal structure of phytase from *Aspergillus ficuum* at 2.5 Å resolution. *Nat. Struct. Biol.* 4 (3), 185–190.
 Liu, X., Han, R., Cao, Y., Turner, B.L., Ma, L.Q., 2022. Enhancing phytate availability in soils and phytate-P acquisition by plants: a review. *Environ. Sci. Technol.* 56 (13), 9196–9219.
 Oh, B.-C., Kim, M.H., Yun, B.-S., Choi, W.-C., Park, S.-C., et al., 2006. Ca(2+)-inositol phosphate chelation mediates the substrate specificity of beta-propeller phytase. *Biochemistry* 45 (31), 9531–9539.
 Potter, S.C., Luciani, A., Eddy, S.R., Park, Y., Lopez, R., Finn, R.D., 2018. HMMER web server: 2018 update. *Nucleic Acids Res.* 46 (W1), W200–W204.
 Puhl, A.A., Gruninger, R.J., Greiner, R., Janzen, T.W., Mosimann, S.C., Selinger, L.B., 2007. Kinetic and structural analysis of a bacterial protein tyrosine phosphatase-like myo-inositol polyphosphatase. *Protein Sci. Publ. Protein Soc.* 16 (7), 1368–1378.
 Rix, G.D., Sprigg, C., Whitfield, H., Hemmings, A.M., Todd, J.D., Brearley, C.A., 2022. Characterisation of a soil MINPP phytase with remarkable long-term stability and activity from *Acinetobacter* sp. *PLoS One* 17 (8), e0272015.
 Schenk, G., Mitić, N., Hanson, G.R., Comba, P., 2013. Purple acid phosphatase: a journey into the function and mechanism of a colorful enzyme. *Coord. Chem. Rev.* 257 (2), 473–482.
 Selle, P.H., Cowieson, A.J., Ravindran, V., 2009. Consequences of calcium interactions with phytate and phytase for poultry and pigs. *Livest. Sci.* 124 (1), 126–141.
 Selle, P.H., Macelline, S.P., Chrystal, P.V., Liu, S.Y., 2023. The contribution of phytate-degrading enzymes to chicken-meat production. *Anim. Open Access J. MDPI.* 13 (4), 603.

- Shin, S., Ha, N.C., Oh, B.C., Oh, T.K., Oh, B.H., 2001. Enzyme mechanism and catalytic property of beta propeller phytase. *Struct. Lond. Engl.* 1993 9 (9), 851–858.
- Shivange, A.V., Schwaneberg, U., 2017. Recent advances in directed phytase evolution and rational phytase engineering. In: Alcalde, M. (Ed.), *Directed Enzyme Evolution: Advances and Applications*. Springer International Publishing, Cham, pp. 145–172.
- Stentz, R., Osborne, S., Horn, N., Li, A.W.H., Hautefort, I., et al., 2014. A bacterial homolog of a eukaryotic inositol phosphate signaling enzyme mediates cross-kingdom dialog in the mammalian gut. *Cell Rep.* 6 (4), 646–656.
- Su, X.B., Ko, A.-L.A., Saiardi, A., 2023. Regulations of *myo*-inositol homeostasis: mechanisms, implications, and perspectives. *Adv. Biol. Regul.* 87, 100921.
- Ullah, A.H., Cummins, B.J., 1988. *Aspergillus ficuum* extracellular pH 6.0 optimum acid phosphatase: purification, N-terminal amino acid sequence, and biochemical characterization. *Prep. Biochem.* 18 (1), 37–65.
- Wyss, M., Brugger, R., Kronenberger, A., Rémy, R., Fimbel, R., et al., 1999. Biochemical characterization of fungal phytases (myo-Inositol hexakisphosphate phosphohydrolases): catalytic properties. *Appl. Environ. Microbiol.* 65 (2), 367–373.
- Yanke, L.J., Bae, H.D., Selinger, L.B., Cheng, K.J., 1998. Phytase activity of anaerobic ruminal bacteria. *Microbiology* 144 (6), 1565–1573.